COMPUTATIONAL MODELLING OF GRADIENT-ENHANCED DAMAGE FOR FRACTURE AND FATIGUE PROBLEMS

R.H.J. Peerlings, R. de Borst[1], W.A.M. Brekelmans and J.H.P. de Vree

Eindhoven University of Technology, Faculty of Mechanical Engineering, The Netherlands

ABSTRACT

Conventional continuum damage descriptions of material degeneration suffer from loss of well-posedness beyond a certain level of accumulated damage. As a consequence, numerical solutions are obtained which are unacceptable from a physical point of view. In this contribution, the introduction of higher-order deformation gradients in the constitutive model is demonstrated to be an adequate remedy to this deficiency of standard damage models. A consistent numerical solution procedure of the governing partial differential equations is presented, which is shown to be capable of properly simulating localization phenomena.

1. INTRODUCTION

Continuum damage models of quasi-brittle failure mechanisms, such as quasi-brittle fracture and fatigue, generally exhibit strain softening. In conventional continuum theories, strain softening is accompanied by the local loss of ellipticity of the differential equations which describe the deformation process. As a consequence, the mathematical description becomes ill-posed and numerical solutions do not converge to a physically meaningful solution upon refinement of the spatial discretization (*e.g.* [1–5]).

Some authors have proposed to abandon the principle of local action in the constitutive relations to remedy the problem of ill-posedness. The so-called non-local continuum models have been postulated to yield physically relevant and mesh-objective solutions [1, 6, 7]. On the other hand, some serious disadvantages of the procedure have been encountered, which

[1]Also Delft University of Technology, Faculty of Civil Engineering, The Netherlands

are a direct consequence of the introduction of non-locality in the mathematical description. Theoretical and practical problems arise in the vicinity of construction edges, particularly if these are of a complex shape, and the construction of a consistent numerical solution procedure requires drastic changes of existing computer codes, while inconsistent tangent operators deteriorate convergence characteristics to a dramatic extent.

As an alternative to non-local softening models, gradient dependent descriptions have gained interest [2, 3, 4, 8, 9, 10]. Although strongly related to non-local theory, gradient dependent models bear the significant advantage of being strictly local in a mathematical sense. The capabilities of gradient dependence have been investigated particularly for plasticity models [3, 8, 9, 10]. A detailed discussion of the incorporation of gradient terms in continuum damage models and the numerical implementation of such descriptions has not been presented hitherto.

In this paper, a gradient formulation of a damage model for quasi-brittle fracture is derived from the non-local theory. As demonstrated by Paas *et al.* [11], the damage model is also capable of describing fatigue phenomena with a slight modification. With regard to numerical solutions, the spatial discretization of the governing equations is discussed and a consistent solution procedure of the resulting equations is presented. The effectiveness of the incorporation of gradient terms in the constitutive description with respect to mesh dependence is demonstrated by a one-dimensional example. Finally, a brief evaluation of the gradient damage model is given.

2. NON-LOCAL MODEL

In this contribution we shall confine ourselves to quasi-brittle materials, which implies that damage evolution is considered to be the dominant dissipative mechanism. Viscous, thermal or other non-mechanical effects are not taken into account and strains and rotations are assumed to be small. Damage is considered to be isotropic; thus a scalar quantity, the damage variable $0 \leq D \leq 1$, suffices to describe the damage process. Undamaged material is characterized by $D = 0$, while $D = 1$ corresponds to complete loss of material coherence.

Here, a strain-based formulation is adopted in the sense of Simo and Ju [12], which, starting from linear elastic material behaviour and utilizing the effective stress concept and the hypothesis of strain equivalence [12], leads to the stress-strain relation

$$\boldsymbol{\sigma} = (1 - D)\, {}^4\boldsymbol{H} : \boldsymbol{\varepsilon}, \tag{1}$$

with $\boldsymbol{\sigma}$ the Cauchy stress tensor, $\boldsymbol{\varepsilon}$ the linear strain tensor and ${}^4\boldsymbol{H}$ the fourth-order Hookean stiffness tensor. The damage state is governed by the scalar history parameter κ, which represents the most severe deformation the material has experienced: $D = D(\kappa)$. In the non-local model, κ is determined by an average scalar measure of the strain, the non-local damage equivalent strain $\overline{\varepsilon}_{eq} \geq 0$, through the Kuhn-Tucker relations

$$\dot{\kappa} \geq 0, \qquad \overline{\varepsilon}_{eq} - \kappa \leq 0, \qquad \dot{\kappa}\,(\overline{\varepsilon}_{eq} - \kappa) = 0 \tag{2}$$

and the initial value $\kappa(0) = \kappa_i$. The value of the non-local equivalent strain $\overline{\varepsilon}_{eq}$ in a certain material point $\vec{x}$ is a weighted average of the local equivalent strains $\varepsilon_{eq} \geq 0$ over the surrounding volume V:

$$\overline{\varepsilon}_{eq}(\vec{x}) = \frac{1}{V}\int_V g(\vec{\xi})\,\varepsilon_{eq}(\vec{x}+\vec{\xi})\,dV, \quad \text{with} \quad \frac{1}{V}\int_V g(\vec{\xi})\,dV = 1, \tag{3}$$

in which $g(\vec{\xi})$ is a weight function and $\vec{\xi}$ denotes the relative position vector pointing to the infinitesimal volume dV.

3. GRADIENT DAMAGE FORMULATION

A gradient formulation can be derived directly from non-local theory [4, 9]. To this end, the local equivalent strain is expanded into a Taylor series according to

$$\begin{aligned}\varepsilon_{eq}(\vec{x}+\vec{\xi}) \;=\; & \varepsilon_{eq}(\vec{x}) + \vec{\nabla}\varepsilon_{eq}(\vec{x})\cdot\vec{\xi} + \frac{1}{2!}\vec{\nabla}^{(2)}\varepsilon_{eq}(\vec{x})\;\cdot^{(2)}\;\vec{\xi}^{(2)} \\ & + \frac{1}{3!}\vec{\nabla}^{(3)}\varepsilon_{eq}(\vec{x})\;\cdot^{(3)}\;\vec{\xi}^{(3)} + \frac{1}{4!}\vec{\nabla}^{(4)}\varepsilon_{eq}(\vec{x})\;\cdot^{(4)}\;\vec{\xi}^{(4)} \\ & + \ldots,\end{aligned} \tag{4}$$

with $\vec{\nabla}^{(n)}$ and $\cdot^{(n)}$ the n^{th} order gradient operator and the n^{th} order inner product respectively; $\vec{\xi}^{(n)}$ designates the n factor dyadic product $\vec{\xi}\vec{\xi}\ldots\vec{\xi}$. With the assumption of isotropy, substitution of (4) into (3) yields

$$\overline{\varepsilon}_{eq} = \varepsilon_{eq} + c\,\nabla^2\varepsilon_{eq} + d\,\nabla^4\varepsilon_{eq} + \ldots, \tag{5}$$

in which the coefficients c, d, ... are determined by the weight function $g(\vec{\xi})$ and the averaging volume V. Thus, neglecting higher order terms in expression (5), definition (3) of the non-local equivalent strain can be replaced by

$$\overline{\varepsilon}_{eq} = \varepsilon_{eq} + c\,\nabla^2\varepsilon_{eq}, \tag{6}$$

with ∇^2 the Laplacian operator (*cf.* [4, 9]). The gradient parameter c in this expression is of the dimension length squared, so that an internal length scale is present in the gradient formulation.

Definition (6) of $\overline{\varepsilon}_{eq}$ is less suitable for numerical analyses. Because of the explicit dependence of $\overline{\varepsilon}_{eq}$ on the Laplacian of the local equivalent strain, finite element elaborations of (6) inevitably lead to $\mathcal{C}^1$-continuity requirements of the displacement [4]. This disadvantage can be avoided as follows. Differentiating expression (5) twice and reordering yields

$$\nabla^2 \varepsilon_{eq} = \nabla^2 \overline{\varepsilon}_{eq} - c\,\nabla^4 \varepsilon_{eq} - d\,\nabla^6 \varepsilon_{eq} + \ldots, \tag{7}$$

substitution of which into (5) leads to

$$\overline{\varepsilon}_{eq} - c\,\nabla^2 \overline{\varepsilon}_{eq} = \varepsilon_{eq} + (d - c^2)\nabla^4 \varepsilon_{eq} + \ldots. \tag{8}$$

Comparing (5) and (8), it can be concluded that employing

$$\overline{\varepsilon}_{eq} - c\,\nabla^2 \overline{\varepsilon}_{eq} = \varepsilon_{eq} \tag{9}$$

as the definition of $\overline{\varepsilon}_{eq}$ will introduce an approximation of the same order of magnitude as the one induced by adopting (6). However, the treatment of $\overline{\varepsilon}_{eq}$ as an independent variable, which has to satisfy the partial differential equation (9), enables a straightforward, $\mathcal{C}^0$-continuous finite element interpolation, as will be shown in the next section.

A difficulty of gradient models that has not been addressed so far, is the requirement of additional boundary conditions. In order to solve the averaging partial differential equation (9), boundary conditions concerning the equivalent strain $\overline{\varepsilon}_{eq}$ have to be specified. From a mathematical point of view, it is necessary to specify either $\overline{\varepsilon}_{eq}$ or the normal derivative $\vec{\nabla}\overline{\varepsilon}_{eq} \cdot \vec{n}$ ($\vec{n}$ denotes the external normal unit vector) in every boundary point of the considered configuration. The physical interpretation of the additional boundary conditions remains a problem. The simple natural boundary condition

$$\vec{\nabla}\overline{\varepsilon}_{eq} \cdot \vec{n} = 0 \tag{10}$$

has been adopted in this paper, in correspondence with [4, 9].

4. FINITE ELEMENT IMPLEMENTATION

The weak forms of the partial differential equations which govern deformation processes are derived according to the weighted residuals approach. The equilibrium equation

$$\vec{\nabla} \cdot \boldsymbol{\sigma} = \vec{0}, \tag{11}$$

in which body forces have not been included for simplicity, is multiplied by the vectorial weight function $\vec{v}(\vec{x})$ and subsequently integrated on the

domain Ω. With the aid of the divergence theorem, the resulting equation can be transformed to the weak form

$$\int_\Omega (\vec{\nabla}\vec{v})^C : \boldsymbol{\sigma}\, d\Omega = \int_\Gamma \vec{v}\cdot\vec{p}\, d\Gamma \qquad \forall\, \vec{v} \in \mathcal{C}^0 \tag{12}$$

of (11), with Γ the configuration boundary and $\vec{p} = \boldsymbol{\sigma}\cdot\vec{n}$ the external stress vector acting on this boundary. The weak form of the averaging equation (9) is obtained in a similar way. Multiplication with the weight function $w(\vec{x})$ and integration yields, again utilizing the divergence theorem and substituting the boundary condition (10),

$$\int_\Omega \left(w\,\overline{\varepsilon}_{eq} + \vec{\nabla} w \cdot c\,\vec{\nabla}\overline{\varepsilon}_{eq} \right) d\Omega = \int_\Omega w\,\varepsilon_{eq}\, d\Omega \qquad \forall\, w \in \mathcal{C}^0. \tag{13}$$

Departing from the weak forms, the finite element discretization is rather straightforward. Following the Galerkin approach, the displacement vector $\vec{u}$ and the weight function $\vec{v}$ are discretized by

$$\vec{u} = \underset{\sim}{\vec{e}}^T \underline{N}\, \underset{\sim}{u}, \qquad \vec{v} = \underset{\sim}{\vec{e}}^T \underline{N}\, \underset{\sim}{v}, \tag{14}$$

with $\underset{\sim}{\vec{e}}$ the vectorial base and the interpolation matrix $\underline{N}$ containing the interpolation polynomials; the columns $\underset{\sim}{u}$ and $\underset{\sim}{v}$ contain the nodal displacement and weight function components, respectively. Taking advantage of the symmetry of $\boldsymbol{\sigma}$, the kernel of the left hand side integral of (12) is elaborated according to

$$(\vec{\nabla}\vec{v})^C : \boldsymbol{\sigma} = \vec{\nabla}\vec{v} : \boldsymbol{\sigma} = \frac{1}{2}\left(\vec{\nabla}\vec{v} + (\vec{\nabla}\vec{v})^C \right) : \boldsymbol{\sigma} = \boldsymbol{b}(\vec{v}) : \boldsymbol{\sigma} \tag{15}$$

and, storing the relevant components of the tensorial strain operator $\boldsymbol{b}$ and the stress tensor $\boldsymbol{\sigma}$ in the arrays $\underset{\sim}{b}$ and $\underset{\sim}{\sigma}$, to

$$(\vec{\nabla}\vec{v})^C : \boldsymbol{\sigma} = \underset{\sim}{b}(\vec{v})^T \underset{\sim}{\sigma} = \underset{\sim}{b}(\underset{\sim}{v})^T \underset{\sim}{\sigma} = \underset{\sim}{v}^T \underline{B}^T \underset{\sim}{\sigma}, \tag{16}$$

with $\underline{B}$ made up of the shape function derivatives. In the right hand side of (12), $\vec{v}\cdot\vec{p}$ is written as

$$\vec{v}\cdot\vec{p} = \underset{\sim}{v}^T \underline{N}^T \underset{\sim}{\vec{e}}\cdot\vec{p} = \underset{\sim}{v}^T \underline{N}^T \underset{\sim}{p}, \tag{17}$$

in which p contains the components of the external load vector $\vec{p}$. Substituting (16) and (17) into (12) and taking into account that the resulting equation is to be satisfied for all $\underset{\sim}{v}$, the customary discrete balance

$$\underset{\sim}{f}^u_{\text{int}} = \underset{\sim}{f}^u_{\text{ext}} \tag{18}$$

of internal and external nodal forces is found, with

$$\underset{\sim}{f}^u_{\text{int}} = \int_\Omega \underline{B}^T \underset{\sim}{\sigma}\, d\Omega, \tag{19}$$

$$\underset{\sim}{f}^u_{\text{ext}} = \int_\Gamma \underline{N}^T \underset{\sim}{p}\, d\Gamma. \tag{20}$$

A separate interpolation of the non-local equivalent strain and the corresponding weight function is introduced:

$$\overline{\varepsilon}_{eq} = \underline{\tilde{N}}\, \underset{\sim}{\overline{\varepsilon}}_{eq}, \qquad w = \underline{\tilde{N}}\, \underset{\sim}{w}, \tag{21}$$

with $\underline{\tilde{N}}$ consisting of interpolation polynomials; $\underset{\sim}{\overline{\varepsilon}}_{eq}$ contains the nodal values of the average equivalent strain and $\underset{\sim}{w}$ those of the weight function w. It is emphasized that the interpolation polynomials of $\vec{u}$ and $\overline{\varepsilon}_{eq}$ need not be of the same order. Both discretizations need to satisfy $\mathcal{C}^0$-continuity requirements. To avoid stress oscillations, the use of an interpolation for the displacements seems advisable which is one order higher than that of the non-local equivalent strains. Using the partial derivative columns

$$\frac{\partial \overline{\varepsilon}_{eq}}{\partial \underset{\sim}{x}} = \underline{\tilde{B}}\, \underset{\sim}{\overline{\varepsilon}}_{eq}, \qquad \frac{\partial w}{\partial \underset{\sim}{x}} = \underline{\tilde{B}}\, \underset{\sim}{w}, \tag{22}$$

the second term in the left hand side of (13) is expanded as

$$\vec{\nabla} w \cdot c\, \vec{\nabla} \overline{\varepsilon}_{eq} = \left(\frac{\partial w}{\partial \underset{\sim}{x}} \right)^T \vec{\underset{\sim}{e}} \cdot c\ \vec{\underset{\sim}{e}}^T \frac{\partial \overline{\varepsilon}_{eq}}{\partial \underset{\sim}{x}} = \underset{\sim}{w}^T \underline{\tilde{B}}^T c\, \underline{\tilde{B}}\, \underset{\sim}{\overline{\varepsilon}}_{eq}. \tag{23}$$

The other terms in (13) are elaborated simply by substitution of (21), leading to

$$\underline{K}^{\varepsilon\varepsilon}\, \underset{\sim}{\overline{\varepsilon}}_{eq} = \underset{\sim}{f}^{\varepsilon}, \tag{24}$$

in which

$$\underline{K}^{\varepsilon\varepsilon} = \int_{\Omega} \left(\underline{\tilde{N}}^T \underline{\tilde{N}} + \underline{\tilde{B}}^T c\, \underline{\tilde{B}} \right) d\Omega, \tag{25}$$

$$\underset{\sim}{f}^{\varepsilon} = \int_{\Omega} \underline{\tilde{N}}^T \varepsilon_{eq}\, d\Omega. \tag{26}$$

With regard to the Newton-Raphson method, which is utilized to solve the discrete equations (18) and (24), the linearized change $\delta \underset{\sim}{\sigma}_i$ of the stress column $\underset{\sim}{\sigma}$ in iteration i is obtained starting from the matrix representation

$$\underset{\sim}{\sigma} = (1 - D)\, \underline{H}\, \underset{\sim}{\varepsilon} \tag{27}$$

of the stress-strain relation (1):

$$\delta \underset{\sim}{\sigma}_i = (1 - D_{i-1})\, \underline{H}\, \delta \underset{\sim}{\varepsilon}_i - \delta D_i\, \underline{H}\, \underset{\sim}{\varepsilon}_{i-1}. \tag{28}$$

For the first right hand side term, application of $\underset{\sim}{\varepsilon} = \underset{\sim}{b}(\underset{\sim}{u}) = \underline{B}\, \underset{\sim}{u}$ simply yields

$$\delta \underset{\sim}{\varepsilon}_i = \underline{B}\, \delta \underset{\sim}{u}_i. \tag{29}$$

The Kuhn-Tucker relations (2) imply that in case of increasing damage ($\dot{\kappa} > 0$) the history parameter satisfies $\kappa = \overline{\varepsilon}_{eq}$, so $\delta\kappa_i = \delta\overline{\varepsilon}_{eq,i}$. If no increase of damage occurs, $\delta\kappa_i$ is given by $\delta\kappa_i = 0$. Whether or not damage is evolving, is determined by the actual value of the non-local equivalent strain compared to the converged value κ_0 of the history parameter in the previous increment. Thus, the change of damage δD_i can be linearized as

$$\delta D_i = q_{i-1}\,\delta\overline{\varepsilon}_{eq,i} = q_{i-1}\,\underline{\tilde{N}}\,\delta\underset{\sim}{\overline{\varepsilon}}_{eq,i}, \tag{30}$$

with

$$q_{i-1} = \begin{cases} \left(\dfrac{\partial D}{\partial \kappa}\right)_{i-1} & \text{if} \quad \overline{\varepsilon}_{eq,i-1} > \kappa_0, \\ 0 & \text{if} \quad \overline{\varepsilon}_{eq,i-1} \leq \kappa_0. \end{cases} \tag{31}$$

With (29) and (30), expression (28) yields

$$\delta\underset{\sim}{\sigma}_i = (1 - D_{i-1})\,\underline{H}\,\underline{B}\,\delta\underset{\sim}{u}_i - \underline{H}\,\underset{\sim}{\varepsilon}_{i-1}\,q_{i-1}\,\underline{\tilde{N}}\,\delta\underset{\sim}{\overline{\varepsilon}}_{eq,i}. \tag{32}$$

so that the iterative change of the internal nodal forces according to (19) may be written as

$$\begin{aligned} \delta\underset{\sim}{f}^{u}_{\text{int},i} \;=\; & \int_{\Omega} \underline{B}^T (1 - D_{i-1})\,\underline{H}\,\underline{B}\,d\Omega \;\; \delta\underset{\sim}{u}_i \\ & - \int_{\Omega} \underline{B}^T \underline{H}\,\underset{\sim}{\varepsilon}_{i-1}\,q_{i-1}\,\underline{\tilde{N}}\,d\Omega \;\; \delta\underset{\sim}{\overline{\varepsilon}}_{eq,i}. \end{aligned} \tag{33}$$

Application of this expression in the discrete equilibrium equation (18) for iteration i leads to

$$\underline{K}^{uu}_{i-1}\,\delta\underset{\sim}{u}_i + \underline{K}^{u\varepsilon}_{i-1}\,\delta\underset{\sim}{\overline{\varepsilon}}_{eq,i} = \underset{\sim}{f}^{u}_{\text{ext}} - \underset{\sim}{f}^{u}_{\text{int},i-1}, \tag{34}$$

with

$$\underline{K}^{uu}_{i-1} = \int_{\Omega} \underline{B}^T (1 - D_{i-1})\,\underline{H}\,\underline{B}\,d\Omega, \tag{35}$$

$$\underline{K}^{u\varepsilon}_{i-1} = -\int_{\Omega} \underline{B}^T \underline{H}\,\underset{\sim}{\varepsilon}_{i-1}\,q_{i-1}\,\underline{\tilde{N}}\,d\Omega. \tag{36}$$

Applying the linearization

$$\delta\varepsilon_{eq,i} = \underset{\sim}{s}^T_{i-1}\delta\underset{\sim}{\varepsilon}_i = \underset{\sim}{s}^T_{i-1}\underline{B}\,\delta\underset{\sim}{u}_i, \tag{37}$$

in which

$$\underset{\sim}{s}_{i-1} = \left(\frac{\partial\varepsilon_{eq}}{\partial\underset{\sim}{\varepsilon}}\right)_{i-1}, \tag{38}$$

equation (24) is elaborated as

$$\underline{K}^{\varepsilon u}_{i-1}\,\delta\underset{\sim}{u}_i + \underline{K}^{\varepsilon\varepsilon}\,\delta\overline{\underset{\sim}{\varepsilon}}_{eq,i} = \underset{\sim}{f}^{\varepsilon}_{i-1} - \underline{K}^{\varepsilon\varepsilon}\,\overline{\underset{\sim}{\varepsilon}}_{eq,i-1}, \tag{39}$$

with $\underline{K}^{\varepsilon\varepsilon}$ and $\underset{\sim}{f}^{\varepsilon}_{i-1}$ according to (25) and (26), respectively, and

$$\underline{K}^{\varepsilon u}_{i-1} = -\int_{\Omega} \underline{\tilde{N}}^{T}\,\underset{\sim}{s}^{T}_{i-1}\,\underline{B}\,d\Omega. \tag{40}$$

The combination of equations (34) and (39) results in a square system of equations

$$\begin{bmatrix} \underline{K}^{uu}_{i-1} & \underline{K}^{u\varepsilon}_{i-1} \\ \underline{K}^{\varepsilon u}_{i-1} & \underline{K}^{\varepsilon\varepsilon} \end{bmatrix} \begin{bmatrix} \delta\underset{\sim}{u}_i \\ \delta\overline{\underset{\sim}{\varepsilon}}_{eq,i} \end{bmatrix} = \begin{bmatrix} \underset{\sim}{f}^{u}_{\text{ext}} \\ \underset{\sim}{f}^{\varepsilon}_{i-1} \end{bmatrix} - \begin{bmatrix} \underset{\sim}{f}^{u}_{\text{int},i-1} \\ \underline{K}^{\varepsilon\varepsilon}\,\overline{\underset{\sim}{\varepsilon}}_{eq,i-1} \end{bmatrix}, \tag{41}$$

which is very similar to the system obtained by De Borst and Mühlhaus [10] for gradient plasticity. Expressions (36) and (40) for the partitions $\underline{K}^{u\varepsilon}_{i-1}$ and $\underline{K}^{\varepsilon u}_{i-1}$ show that the tangent stiffness matrix is non-symmetric.

5. EXAMPLE

The merits of the gradient damage formulation are demonstrated using a simple, one-dimensional test problem. A bar of length L is considered (Figure 1), which is subjected to a uniaxial, pure tension loading. While

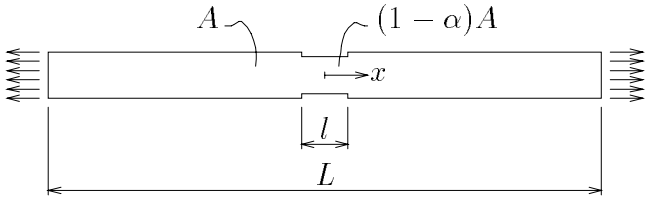

Figure 1: One-dimensional test configuration.

all material characteristics are uniform for the entire bar, the cross sectional area A has been reduced by a factor $(1-\alpha)$ between $x = -\frac{1}{2}l$ and $x = \frac{1}{2}l$ in order to trigger localization of deformation. If the damage evolution law is chosen such that it represents the damage equivalent of perfect plasticity, an analytical solution can be constructed for this problem. Numerical solutions appear to converge to this analytical solution upon mesh refinement [13]. Here, the evolution law is chosen as

$$D(\kappa) = \begin{cases} \dfrac{\kappa_c}{\kappa}\dfrac{\kappa-\kappa_i}{\kappa_c-\kappa_i} & \text{if } \kappa_i \le \kappa \le \kappa_c, \\ 1 & \text{if } \kappa > \kappa_c, \end{cases} \tag{42}$$

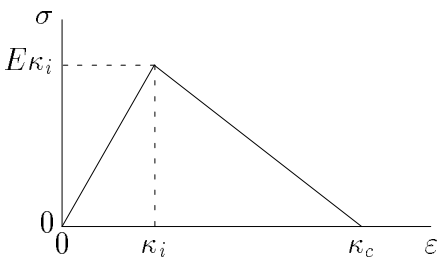

Figure 2: Local damage model response.

which yields a linear softening stress-strain relation in a local damage formulation (Figure 2). The length and cross sectional area of the bar are taken equal to $L = 100\,\mathrm{mm}$ and $A = 10\,\mathrm{mm}^2$, respectively. The length l of the weakened zone is set equal to $l = 10\,\mathrm{mm}$, the cross section reduction factor to $\alpha = 0.1$. Young's modulus is chosen as $E = 20{,}000\,\mathrm{N/mm}^2$, while the initial and critical value of the history parameter are set equal to $\kappa_i = 10^{-4}$ and $\kappa_c = 0.0125$, respectively.

For a reference value $c = 1\,\mathrm{mm}^2$ of the gradient parameter, numerical solutions have been computed employing 80, 160, 320 and 640 element discretizations. Quadratic interpolation polynomials have been used for the displacements and linear polynomials for the non-local equivalent strain. The load-deflection curves obtained with these meshes have been plotted in Figure 3. They show a clear convergence to a meaningful, softening solution with a finite energy dissipation.

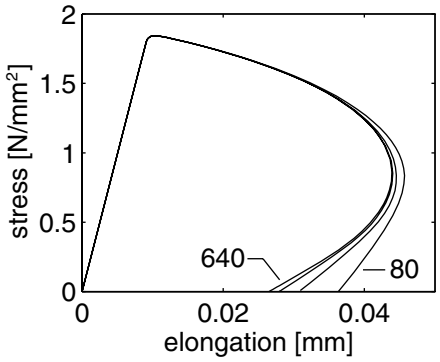

Figure 3: Load-deflection curves for 80, 160, 320 and 640 element meshes.

In Figure 4, the strain and damage evolution have been plotted for the 640 element mesh. The formation of an initially relatively large damaged area (Figure 4(b)) and the subsequent development of a narrow region of intense deformation (Figure 4(a)), seems to be an appropriate description

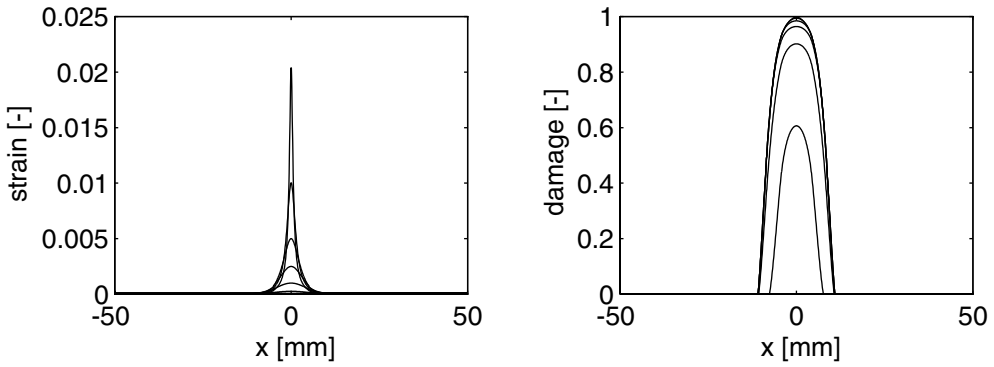

(a) strain (b) damage

Figure 4: Strain and damage evolution.

of the process of initiation and growth of microcracks in a relatively wide area and coalescence of some of these microcracks into one macrocrack.

To examine the effect of gradient parameter variations on the response, the 640 element simulation has been repeated for $c = 0.25$, 0.50, 1.00, 2.00 and 4.00 mm^2. In Figure 5(a), the stress in the bar has been plotted versus its elongation for $c = 0.25, 1.00$ and $4.00\,\mathrm{mm}^2$. The less brittle behaviour

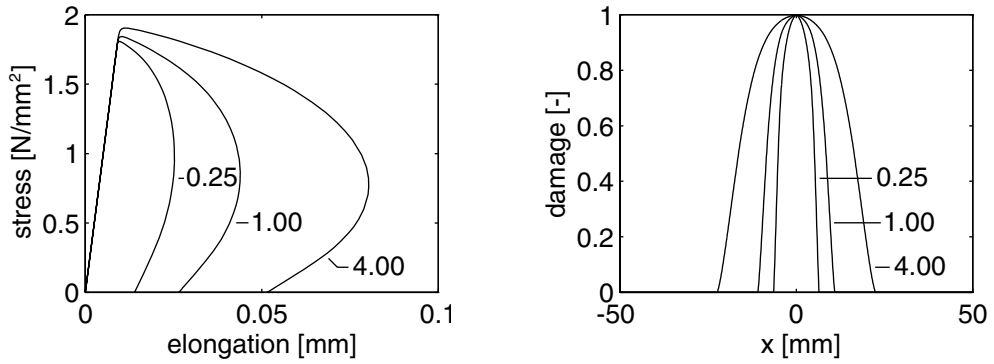

(a) stress (b) damage

Figure 5: Responses for $c = 0.25, 1.00$ and $4.00\,\mathrm{mm}^2$.

for higher values of c, which is observed in this plot, can be related to the damage profiles at the moment of complete rupture (Figure 5(b)). For higher values of c, and thus for a larger internal length, damage localizes in a larger region, and as a consequence larger elongations are encountered. The dependence of the width of the damaged zone on the internal length $\sqrt{c}$, is demonstrated in Figure 6(a). Another interesting relation is that between the internal length scale and the energy which is dissipated in the

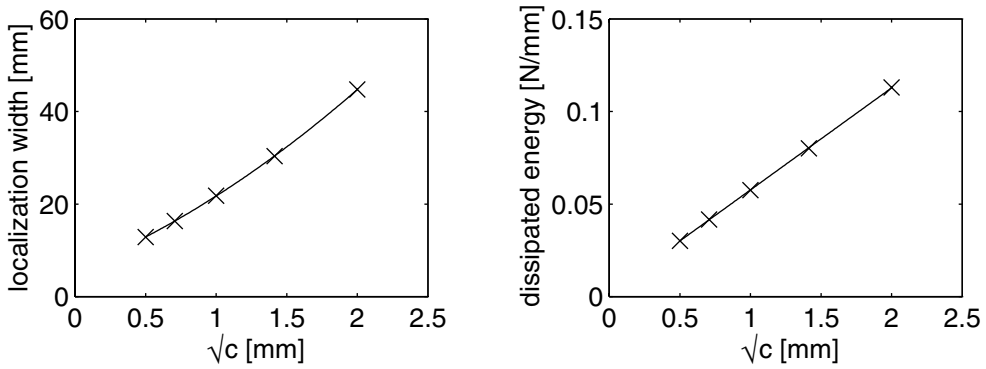

(a) localization width (b) dissipated energy

Figure 6: Influence of gradient parameter on localization width and dissipated energy.

fracture process. Figure 6(b) shows that the dependence of the dissipated energy on the internal length is linear in the gradient model.

6. CONCLUSION

The merits of gradient dependence with respect to localization phenomena have been shown in the context of continuum damage mechanics. The inclusion of a second order gradient term in the mathematical description of material behaviour implicitly introduces an internal length in the constitutive model. On the occurrence of softening, the width of the zone in which deformation is localized is determined by this internal length scale, as has been demonstrated by a simple, one-dimensional example.

The gradient dependent continuum damage model for quasi-brittle materials has been derived from non-local theory. The averaging procedure which forms a part of the non-local model, has been replaced by a partial differential equation, which has to be solved in addition to the equilibrium equation. As a consequence, the 'non-local' scalar measure of strain which governs damage evolution is considered as an additional independent variable. From the mathematical viewpoint, boundary conditions with regard to damage evolution can be incorporated in a natural fashion. For numerical solutions, the independent variables are interpolated separately. As a result of the implicit incorporation of the gradient term, both discretizations need to satisfy only $\mathcal{C}^0$-continuity. A consistent solution strategy for the resulting equations has been derived, which conforms to standard finite element procedures.

REFERENCES

[1] Bažant, Z.P., Belytschko, T., and Chang, T.P. Continuum theory for strain-softening. J. Eng. Mech., 110, 1666–1692, 1984.

[2] Triantafyllidis, N. and Aifantis, E.C. A gradient approach to localization of deformation: I. Hyperelastic materials. J. Elasticity, 16, 225–237, 1986.

[3] Schreyer, H.L. and Chen, Z. One-dimensional softening with localization. J. Appl. Mech., 53, 791–797, 1986.

[4] Lasry, D. and Belytschko, T. Localization limiters in transient problems. Int. J. Solids Structures, 24, 581–597, 1988.

[5] de Borst, R., Sluys, L.J., Mühlhaus, H.-B., and Pamin, J. Fundamental issues in finite element analysis of localization of deformation. Eng. Comp., 10, 99–121, 1993.

[6] Bažant, Z.P. and Pijaudier-Cabot, G. Nonlocal continuum damage, localization instability and convergence. J. Appl. Mech., 55, 287–293, 1988.

[7] de Vree, J.H.P., Brekelmans, W.A.M., and van Gils, M.A.J. Comparison of nonlocal approaches in continuum damage mechanics. Accepted for publication in Computers & Structures.

[8] Aifantis, E.C. On the microstructural origin of certain inelastic models. J. Eng. Mat. Technol., 106, 326–330, 1984.

[9] Mühlhaus, H.-B. and Aifantis, E.C. A variational principle for gradient plasticity. Int. J. Solids Structures, 28, 845–857, 1991.

[10] de Borst, R. and Mühlhaus, H.-B. Gradient-dependent plasticity: formulation and algorithmic aspects. Int. J. Num. Meth. Eng., 35, 521–539, 1992.

[11] Paas, M.H.J.W., Schreurs, P.J.G., and Brekelmans, W.A.M. A continuum approach to brittle and fatigue damage: theory and numerical procedures. Int. J. Solids Structures, 30, 579–599, 1993.

[12] Simo, J.C. and Ju, J.W. Strain- and stress-based continuum damage models: I. Formulation. Int. J. Solids Structures, 23, 821–840, 1987.

[13] Peerlings, R.H.J., de Borst, R., Brekelmans, W.A.M., and de Vree, J.H.P. Gradient-enhanced damage for quasi-brittle materials. In preparation.